

Probing the formation of dark interlayer excitons via ultrafast photocurrent

Denis Yagodkin¹, Elias Ankerhold¹, Abhijeet Kumar¹, Johanna Richter¹,

Kenji Watanabe², Takashi Taniguchi³, Cornelius Gahl¹, and Kirill I. Bolotin^{1*}

¹*Department of Physics, Freie Universität Berlin, Arnimallee 14, Berlin 14195, Germany*

²*Research Center for Functional Materials, National Institute for Materials Science, 1-1 Namiki, Tsukuba 305-0044, Japan and*

³*International Center for Materials Nanoarchitectonics,*

National Institute for Materials Science, 1-1 Namiki, Tsukuba 305-0044, Japan

(Dated: March 1, 2023)

Optically dark excitons determine a wide range of properties of photoexcited semiconductors yet are hard to access via conventional spectroscopies. Here, we develop a time-resolved ultrafast photocurrent technique (trPC) to probe the formation dynamics of optically dark excitons. The nonlinear nature of the trPC makes it particularly sensitive to the formation of excitons occurring at the femtosecond timescale after the excitation. As proof of principle, we extract the interlayer exciton formation time 0.4 ps at 160 $\mu\text{J}/\text{cm}^2$ fluence in a MoS₂/MoSe₂ heterostructure and show that this time decreases with fluence. In addition, our approach provides access to the dynamics of carriers and their interlayer transport. Overall, our work establishes trPC as a technique to study dark excitons in various systems that are hard to probe by other approaches.

Coulomb-bound electron-hole pairs (excitons) dominate the optical response of 2D semiconductors from the group of transitional metal dichalcogenides (TMDs) [1]. While early studies focused on optically allowed bright excitons, optically forbidden "dark" excitons are much less studied. The radiative recombination of these latter excitons is suppressed as they involve states with non-zero total momentum, non-integer total spin, or spatially separated electron and hole wavefunctions [1, 2]. Due to the weak interaction with light, these states have a long lifetime. Dark excitons are also the lowest energy excitation in many TMDs [3]. Because of that, dark exciton states likely dominate the long-range transport of excitons [4, 5], determine temperature-dependent optical spectra [6], and are responsible for long-lived spin signals in TMDs [7, 8]. Furthermore, dark excitons are promising for realizing interacting bosonic many-body states including the Bose-Einstein condensate and excitonic Mott insulator [9–11].

Special approaches are required to investigate the properties of the dark states due to their weak interaction with light. For example, time- and angle-resolved photoemission spectroscopy (trARPES) or spectroscopies in the terahertz and far-infrared frequency ranges have been used to study dark excitons in TMDs and their heterostructures (HS) [12–14]. These approaches typically require large (hundreds of μm^2 area) homogenous samples or are performed at room temperature. Another approach to probe dark excitons, time-resolved photoluminescence (trPL) [10, 15], has a submicron spatial resolution but features a lower time resolution and does not work for states with vanishingly small oscillator strengths. As a result, many questions related to dark exciton formation, e.g. its timescale or the influence of phonon scattering and electron screening, remain unresolved.

Time-resolved photocurrent spectroscopy (trPC) has recently emerged as an approach to study optical processes in (2D) semiconductors [16–19]. In trPC, a current across the sample is recorded vs. the time delay between two light pulses impinging onto it. Critically, the technique is inherently sensitive to nonlinear processes. The approach applies to devices down to the nm-scale and is compatible with other probes such as magnetic or electric fields, temperature, or strain. Finally, as a transport-based technique, trPC is inherently sensitive to the phenomena at contacts and interfaces. Here, we use the non-linear response of two-color trPC to probe the formation dynamics of dark excitonic species. To test our approach, we interrogate the formation dynamics of the the most studied dark excitons in TMDs: interlayer excitons in MoS₂/MoSe₂ heterostructures.

Toy model of time-resolved photocurrent. Our first goal is to show that the dynamics of dark excitons, which are not accessible to conventional optical techniques, can be obtained from the time-dependent populations of free carriers. To understand this, we consider a simplified model of an optically excited semiconductor. We track the time-dependent densities of free electrons $N_e(t)$ and free holes $N_h(t)$. We assume that electron and hole populations can be excited together (direct excitation) or separately (indirect excitation), which we model by generation functions $G_e(t)$ and $G_h(t)$. We focus on coupled relaxation $\sim N_e N_h$ which describes the binding of an electron and a hole into an exciton [20] (other terms are analyzed in the Supplementary Note 1). Overall, the carrier populations are described within our toy model by the following equations:

$$\begin{cases} \frac{dN_e}{dt} = -\frac{N_e}{\tau_e} - \gamma_{e-h} N_e N_h + G_e \\ \frac{dN_h}{dt} = -\frac{N_h}{\tau_h} - \gamma_{e-h} N_e N_h + G_h \end{cases} \quad (1)$$

Here $\tau_{e/h}$ are linear decay times of electron and hole

* kirill.bolotin@fu-berlin.de

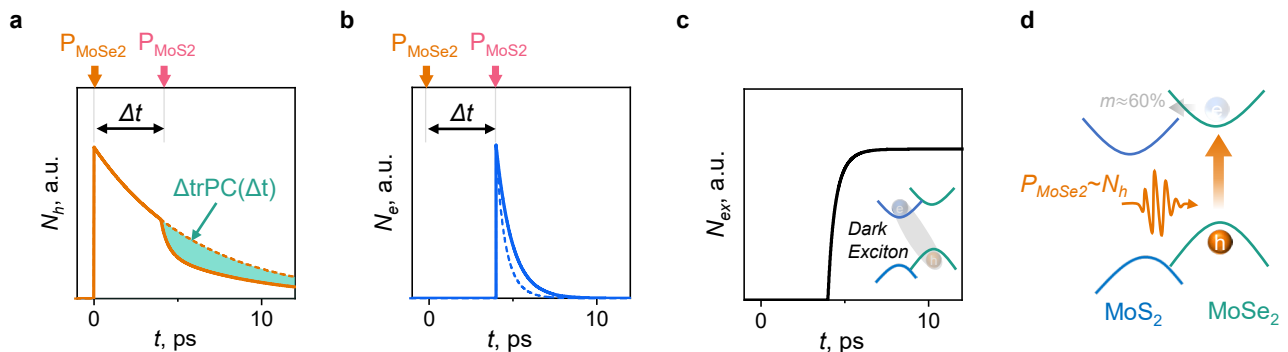


FIG. 1. **Excitation dynamics and photocurrent.** **a-c)** Dynamics of holes (a), electrons (b) and excitons (c) modelled by Eq. 1. Solid and dashed lines correspond to non-zero and zero exciton formation rate (γ_{e-h}). After the excitation by a pulse resonant with the MoSe₂ bandgap (P_{MoSe_2}) at $t = 0$, the hole population (N_h) decays exponentially with the rate τ_h . This decay is accelerated after electrons are excited (P_{MoS_2}) at $\Delta t \approx \tau_h = 4$ ps in the case $\gamma_{e-h} \neq 0$. The quantitative measure of this acceleration, the shaded area in a, is on the one hand determined by γ_{e-h} and on the other hand can be detected in a time-resolved photocurrent (trPC) experiment. **d)** An optical pump pulse in resonance with MoSe₂ bandgap (P_{MoSe_2}) excites predominantly holes in the VBM of the heterostructure, while MoS₂ resonant pulse excites electrons in CBM (not shown). Binding of electron and hole in individual layers yields dark interlayer excitons (Inset in c).

populations, and γ_{e-h} is the nonlinear exciton formation rate. Since the decay of excitons is several orders of magnitude slower compared to the decay/trapping of free electrons and holes [21, 22], the density of the excitons is given by

$$N_{ex}(t) = \int_{-\infty}^t \gamma_{e-h} N_e N_h dt^*.$$

While the excitons described by $N_{ex}(t)$ can be dark (and hence hard to probe), it can be reconstructed if we have experimental access to $N_e(t)$ and $N_h(t)$. To accomplish this, we numerically solve the above equations for parameters typical for TMD materials (see SI for details). For simplicity, we first assume that holes and electrons can be excited separately. When only holes are excited at $t_1 = 0$ ps and only electrons at, for example, $t_2 \approx \tau_h = 4$ ps, the solution yields dynamics shown in Fig. 1a-c. Initially, the excited population of holes decays exponentially. After the second pulse arrives, electrons are generated (Fig. 1b). The decay of holes speeds up due to the formation of excitons if γ_{e-h} is non-zero. Interestingly, we see that the population of excitons (Fig. 1c) qualitatively follows the difference between the hole populations with zero and non-zero γ_{e-h} (dashed and solid lines in Fig. 1a). For the non-interacting case ($\gamma_{e-h} = 0$), the hole density is not affected by the second pulse exciting electrons (as in a single pulse excitation case) and therefore the population of excitons can also be equated to the difference of hole densities between a single pulse excitation ($G_h \neq 0$; $G_e = 0$) vs. two pulse excitation ($G_h \neq 0$; $G_e \neq 0$). We see that, in principle, the dynamics of dark excitons can be obtained from the dynamics of free carriers.

Two obvious challenges arise when applying this toy model to a realistic physical system. First, conven-

tional optical techniques, such as transient reflectivity, detect combined contributions from photoexcited electron (N_e), hole (N_h), and exciton (N_{ex}) populations. Second, in conventional semiconductors, optical pulses generate electrons and holes simultaneously, so the generation functions G_h and G_e cannot be separately controlled.

To address the first problem, we use time-resolved photocurrent spectroscopy as our measurement technique. Generally, photocurrent spectroscopies have the advantage of being directly sensitive to photogenerated electrons/holes while being insensitive to (neutral) excitons [17, 18]. In trPC, the system is illuminated by two optical pulses separated by the time interval Δt : $G_h(t_0)$ and $G_e(t_0 + \Delta t)$, which generate populations of N_h^0 and N_e^0 , respectively. The DC current across the material is recorded. The trPC signal is defined as the difference in current with both pulses being present versus only a single pulse. In general, photocurrent is proportional to the total amount of free carriers generated in a system over time. For the systems under study, TMDs, the direct contribution of electrons to the photocurrent can be neglected as their lifetime is much lower and contact resistance is higher than holes [17, 23] (see Supplementary Note 1). In that case, the photocurrent produced by only the first pulse is given by the area under the dashed orange curve in Fig. 1a. The decay of the hole population, in this case, depends only on τ_h as $G_e = 0$ for single pulse excitation. The same holds for $\gamma_{e-h} = 0$ since the nonlinear term in Eq. 1 vanishes for both cases. The photocurrent produced by two pulses is given by the area under the solid curve in Fig. 1a and is smaller than that of a single pulse because of holes recombining with photoexcited electrons. It can be shown analytically (Supplementary Note 4) that in the limit of small γ_{e-h} and $\tau_h \gg \tau_e$, the trPC scales linearly with the exciton formation rate,

$$\Delta \text{trPC}(\Delta t) \sim \gamma_{e-h} N_e^0 N_h^0 \tau_e \tau_h \cdot \exp\left(-\frac{\Delta t}{\tau_{e/h}}\right) \quad (2)$$

Here the decay time (denominator in the exponent) is τ_h if holes are excited first (positive delay time $\Delta t > 0$) and τ_e if electrons are excited first (negative delay time $\Delta t < 0$). To summarize, trPC can be used to measure both free carrier parameters (τ_e, τ_h) as well as the exciton formation rate (γ_{e-h}).

To address the second problem, we use a 2D heterostructure $\text{MoS}_2/\text{MoSe}_2$ as a system where the generation rates for electrons and holes can be controlled separately. Indeed, the conduction band minimum (CBM) and valence band maximum (VBM) of the heterostructure reside in different materials, MoS_2 and MoSe_2 respectively (Fig. 1d). Because of that, an optical pulse in resonance with e.g., MoSe_2 bandgap (P_{MoSe_2}) excites holes in the VBM of the structure (MoSe_2), while the excited electrons can relax to the CBM (MoS_2) through tunneling. Crucially, only around $m \approx 60\%$ of these electrons reach the CBM of the structure in MoS_2 [24] (Fig. 1d). The remaining electrons are trapped and do not contribute to photocurrent [25, 26]. These electrons are not affected by the second pulse [27]. Similarly, a pulse resonant with MoS_2 bandgap (P_{MoS_2}) excites electrons in CBM while $m \approx 60\%$ of holes reach VBM of the structure. We see that the excitation of MoSe_2 produces predominantly free holes, while the excitation of MoS_2 produces predominantly free electrons.

We now apply Eq. 1 to model the excitation dynamics of the $\text{MoS}_2/\text{MoSe}_2$ heterostructure. The parameter $N_e(t)$ describes the electron density in the CBM of the structure (MoS_2) and $N_h(t)$ – the hole density in the VBM (MoSe_2). The free electron/hole decay time (the term linear with $N_{e/h}$) describes the combined contributions of defect capture [28], intervalley scattering [29], and radiative decay processes [25, 26]. The rate γ_{e-h} describes the formation of (dark) interlayer excitons. Of course, intralayer excitons are also formed by optical pulses. However, optically excited intralayer excitons decay much faster (within < 100 fs [12]) compared to intralayer exciton recombination ($> \text{ps}$) and electron/hole population cooling rate [30–32] via charge separation across the heterostructure and are therefore subsume in the generation functions G_e and G_h . The latter contain contributions from both pulses (i.e., $G_e(t) = P_{\text{MoS}_2}(t, t_0) + m \cdot P_{\text{MoSe}_2}(t, t_0 + \Delta t)$, see effect of m on dynamics of charge carriers in Fig. S5). Finally, the excitonic ground state of $\text{MoS}_2/\text{MoSe}_2$ is an interlayer exciton comprised of an electron in MoS_2 bound to a hole in MoSe_2 (Fig. 1f). When the twist angle between the heterostructure layers (θ) is non-zero, the interlayer exciton has large in-plane momentum: $k \sim \frac{\theta}{a}$, where a is the averaged lattice constant of the heterostructure [33, 34]. In this case, the radiative recombination must involve a phonon and the state is dark [34]. Thus, the interlayer exciton decay (> 100 ps) can be neglected on the time

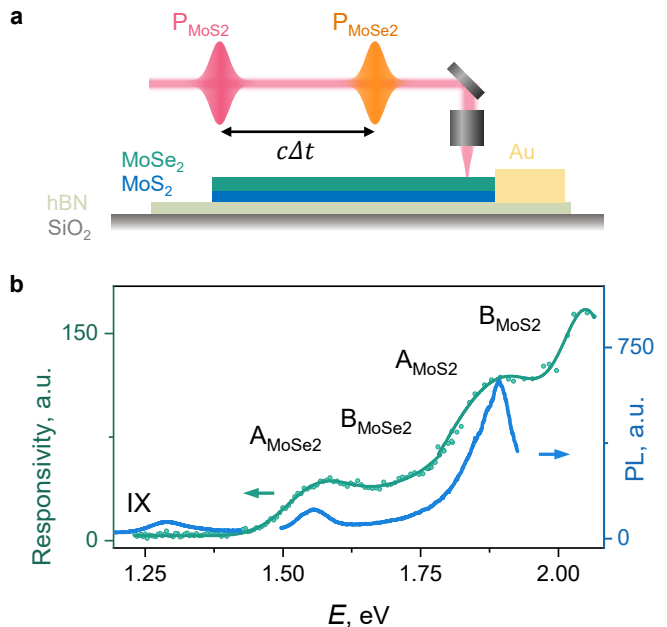


FIG. 2. **Sample structure and measurement techniques.** **a)** Scheme of two-color time-resolved photocurrent measurements (trPC). A photocurrent excited in the TMD heterostructure is measured vs. time delay between a pulse in resonance with MoSe_2 (P_{MoSe_2}) and a pulse in resonance with MoS_2 (P_{MoS_2}). **b)** Photocurrent responsivity (green dots, left axis) and PL (blue line, right axis) spectra of $\text{MoS}_2/\text{MoSe}_2$ heterostructure. Intralayer A and B excitons of MoS_2 , MoSe_2 are seen (solid green fit) in PC at bias voltage of 3.0 V. In PL, an additional feature, an interlayer exciton (IX) is observed.

scales of the population build-up [35]. Our next goal is to obtain the dynamics of $N_{ex}(t)$ via trPC.

Time-resolved photocurrent. For trPC measurements, we fabricate samples, $\text{MoS}_2/\text{MoSe}_2$ on hBN, (Fig. 2a; see Supplementary Note 2 for details). We observe the characteristic intralayer A and B excitons for both materials in static photocurrent spectroscopy in the heterostructure region (green dots in Fig. 2b and Fig. S1). In addition, weak photoluminescence (PL) due to interlayer excitons (IX) is observed at 1.3 eV [36] (blue line in Fig. 2b). For time-resolved photocurrent (trPC) measurements, the sample is illuminated with two time-relayed (with ~ 10 fs precision) optical pulses, one in resonance with the MoS_2 bandgap and another with the MoSe_2 bandgap. The photocurrent is measured with lock-in amplifier synchronized to an optical chopper in one of the beam paths with no bias voltage applied. This measurement effectively allows us to evaluate the difference between single- and two-pulse responses, which corresponds to the area between dashed and solid curves in Fig. 1a.

Figure 3a shows experimental trPC data (green dots) of the $\text{MoS}_2/\text{MoSe}_2$ sample vs. delay Δt between the excitation pulses. Positive delay corresponds to the pulses resonant with the MoS_2 bandgap arriving first. The most

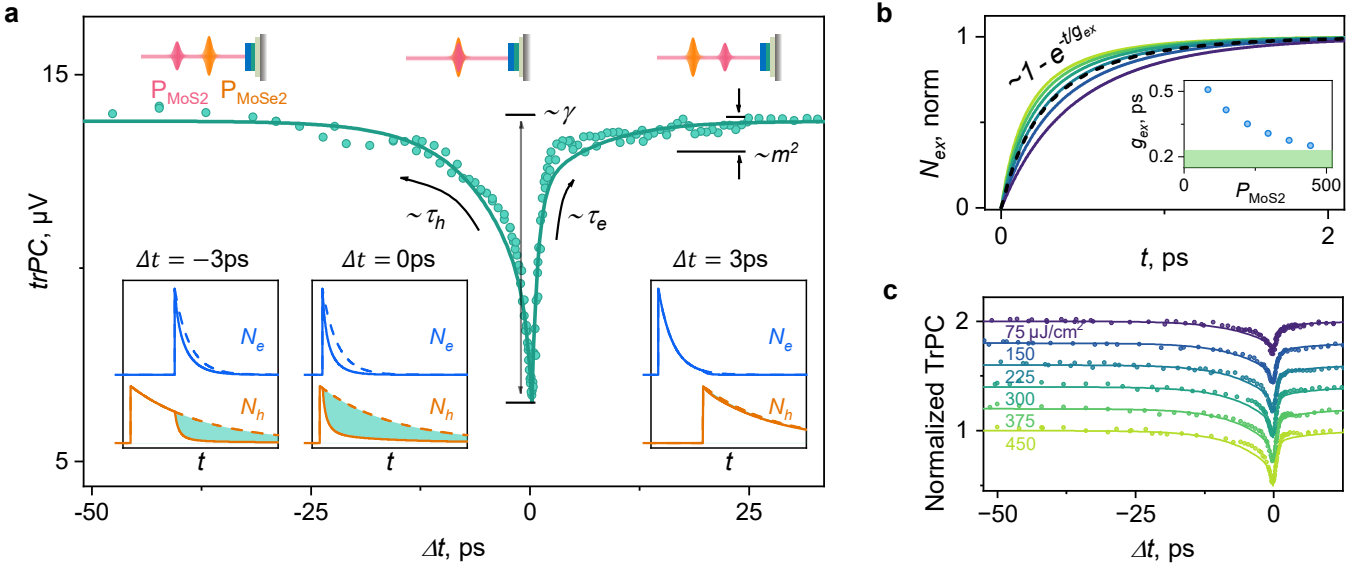


FIG. 3. **trPC measurements and extraction of exciton dynamics.** **a)** trPC response of a $\text{MoS}_2/\text{MoSe}_2$ heterostructure (points). Solid line shows simulated dynamics from Eq. 1 model with following parameters: $\tau_e = 1.0$ ps, $\tau_h = 6.0$ ps, interaction strength $\gamma_{e-h} = 0.13$ cm^2/s , electron/hole tunneling $m = 55\%$. The insets display dynamics of holes (orange) and electrons (blue) for selected delays between pulses for the simplified case $m = 0$. The difference between response to a single optical pulse (solid) and two pulses (dashed) is proportional to Δt trPC (green area). **b)** Simulated dynamics of interlayer excitons formation for data in a (black dashed line) and for other fluences $P_{\text{MoS}_2} = 75, 150, 225, 300, 375, 450$ $\mu\text{J}/\text{cm}^2$ (solid lines from purple to yellow). For higher fluences exciton formation becomes faster, as quantified by fitting to $1 - e^{-t/g_{ex}}$, where g_{ex} is the exciton formation time. Inset: extracted g_{ex} for the above mentioned fluence range (blue points), green area shows cross correlation of the pulses. The formation time drastically decreases for high laser fluences. **c)** Normalized fluence dependence of trPC response (points, each dataset is offset by 0.25) and independent from measurement simulations using Eq. 1 with parameters from Fig. 3a (lines). At higher fluences (yellow) the trPC drop at zero-time delay increases, suggesting faster formation and higher number of excitons.

prominent features of the data are a strong dip at zero time delay and a pronounced asymmetry between positive and negative delays. We now show that these features can be understood within our toy model. First, a large drop in trPC suggests non-linear interaction between the carrier populations produced by both pulses, described by γ_{e-h} in our model (Eq. 2). Second, the asymmetry can be understood from Eq. 2. It suggests that the lifetime of electrons photoexcited in MoS_2 is much smaller than the lifetime of holes excited in MoSe_2 (see insets in Fig. 3a for the illustration of trPC at negative, zero, and positive time delays). Third, we note a slower decaying component at $\Delta t > 3$ ps. This minor effect is missing in Fig. 1a and occurs for $m \neq 0$ (Supplementary Note 5). Its origin is the transfer of holes to the VBM (MoSe_2). The ratio between fast and slow decaying components is proportional to m^2 (Eq. S12).

To obtain the precise values of the model parameters, we match the numerical solution of Eq. 1 (the solid line in Fig. 3a) with the experimental data. We obtain decay times $\tau_h = 6.0 \pm 0.5$ ps, $\tau_e = 1.0 \pm 0.2$ ps, interaction strength $\gamma_{e-h} = 0.13 \pm 0.04$ cm^2/s , and transfer efficiency $m = 55 \pm 5\%$. The effect of every parameter is shown in Fig. S7. Using the extracted parameters, we plot the generation dynamics of interlayer excitons (black dashed line in Fig. 3b). Since the exciton formation is a nonlinear

process, its acceleration is expected with a higher density of electrons/holes which matches simulations at higher fluence (solid lines Fig. 3b). We also extract the dynamics of electrons and holes transferred after photoexcitation within our model (Fig. S2a). These transferred carriers can be measured with two-color time-resolved reflectivity (trRef) measurements (Supplementary Note 3). Overall, the simulations suggest two key behaviors. First, we see a much faster decay rate for electrons compared to holes. Second, we obtain a formation time of the exciton, $g_{ex} = 0.4$ ps, at our experimental incident fluence $P_{\text{MoS}_2} = 160$ $\mu\text{J}/\text{cm}^2$. This time is expected to be strongly fluence dependent, dropping by a factor of three for tripled fluence of P_{MoS_2} (inset in Fig. 3b).

Next, we test the predictions of these simulations. To independently check the dynamics of free carriers, we carry out two-color time-resolved reflectivity [22] (Supplementary Note 3). The resulting time constants of electrons and holes, $\tau_e = 1.4$ ps and $\tau_h = 6.3$ ps, are close to what is obtained from trPC. Moreover, our model for trRef suggests that the formation of dark excitons is the reason behind the bi-exponential decay observed by us and in other works [22, 23]. To check the dependence of exciton formation on fluence given by our model (Fig. 3b), we carried out fluence-dependent trPC measurements. We keep the incident fluence of P_{MoSe_2}

fixed, while P_{MoS_2} is varied in the range used in simulation: $75 \mu\text{J}/\text{cm}^2 - 450 \mu\text{J}/\text{cm}^2$ (dots in Fig. 5). We see that the magnitude of the drop of the trPC at zero time delay increases with fluence, from around 30% at $75 \mu\text{J}/\text{cm}^2$ up to 50% at $450 \mu\text{J}/\text{cm}^2$. The experimental data closely follow the independent predictions of the model (lines in Fig. 3c) where we used the same parameters as Fig. 3a and only changed the fluence of the beams. We extract the formation time of interlayer excitons g_{ex} (inset in Fig. 3b) and find that it is more than halved in the given fluence range from 0.5 ps to 0.2 ps.

Conclusion and outlook. To summarize the discussion above, the proposed model matches all observed features of the trPC behavior. We extract the parameters of the model: e-h coupling ($\gamma_{e-h} = 0.13 \pm 0.04 \text{ cm}^2/\text{s}$), decay times of electrons and holes ($\tau_e = 1.0 \pm 0.2 \text{ ps}$ and $\tau_h = 6.0 \pm 0.5 \text{ ps}$), and efficiency of interlayer transport ($m = 55 \pm 5\%$), for all fluence regimes. The interlayer exciton formation time varies from 0.2 ps to 0.5 ps in the range of fluences $450 \mu\text{J}/\text{cm}^2$ to $75 \mu\text{J}/\text{cm}^2$. It is useful to compare these values with those obtained by other approaches. Electron/hole lifetimes are consistent with those broadly reported from optical measurements [7, 25, 32, 37, 38]. The shorter lifetime of electrons is likely related to defect states being closer to the conduction band [39, 40]. The observed exciton formation time $g_{ex} = 0.4 \text{ ps}$ at $160 \mu\text{J}/\text{cm}^2$ fluence matches the time scales reported in trARPES ($\sim 230 \text{ fs}$) [12], trTHz reflectivity ($\sim 350 \text{ fs}$) [41], and trFIR ($\sim 800 \text{ fs}$) [42] experiments. The interlayer transfer efficiency m has been estimated from THz measurements to be 50–70% [24], also close to the values here. Overall, our approach provides simple access to the dynamics of (dark) interlayer excitons. Moreover, the proposed model describes trRef dynamics of heterostructures and explains the biexpo-

ponential decay reported before [22, 23].

To conclude, we demonstrate an approach for studying dark exciton formation dynamics. In future, this approach can be used to study other dark excitons in TMDs. Unlike other approaches, trPC is fully compatible with other optical techniques (trRef and PL shown here, Kerr and ellipticity spectroscopies, second harmonic generation), has hundreds of nanometers spatial resolution, and works at cryogenic temperatures. It will be particularly interesting to use trPC to uncover the effects of many-body interaction (exciton Mott transition, localization at low temperature), electric field, and twist angle on the exciton formation time.

Acknowledgment

The authors thank Nele Stetzuhn for her comments on the paper. The authors acknowledge the German Research Foundation (DFG) for financial support through the Collaborative Research Center TRR 227 Ultrafast Spin Dynamics (project B08).

Conflict of Interest

The authors declare no conflict of interest.

Author Contribution

D.Y., K.I.B., and C.G. conceived and designed the experiments, D.Y., E.A., A.K., and J.R. prepared the samples, D.Y., A.K. and E.A. performed the optical measurements, D.Y. analyzed the data, E.A. wrote software for simulations, D.Y., E.A., performed the calculations and help to rationalize the experimental data, D.Y. and K.I.B. wrote the manuscript with input from all co-authors.

Data Availability Statement

The data that support the findings of this study are available from the corresponding author upon reasonable request.

-
- [1] G. Wang, A. Chernikov, M. M. Glazov, T. F. Heinz, X. Marie, T. Amand, and B. Urbaszek, *Colloquium* : Excitons in atomically thin transition metal dichalcogenides, *Reviews of Modern Physics* **90**, 021001 (2018-04-04).
 - [2] T. Mueller and E. Malic, Exciton physics and device application of two-dimensional transition metal dichalcogenide semiconductors, *npj 2D Materials and Applications* **2**, 29 (2018-12-10).
 - [3] E. Malic, M. Selig, M. Feierabend, S. Brem, D. Christiansen, F. Wendler, A. Knorr, and G. Berghäuser, Dark excitons in transition metal dichalcogenides, *Physical Review Materials* **2**, 014002 (2018-01-17).
 - [4] R. Rosati, R. Schmidt, S. Brem, R. Perea-Causín, I. Niehues, J. Kern, J. A. Preuß, R. Schneider, S. Michaelis de Vasconcellos, R. Bratschitsch, and E. Malic, Dark exciton anti-funneling in atomically thin semiconductors, *Nature Communications* **12**, 7221 (2021-12-10).
 - [5] R. Rosati, S. Brem, R. Perea-Causín, R. Schmidt, I. Niehues, S. Michaelis de Vasconcellos, R. Bratschitsch, and E. Malic, Strain-dependent exciton diffusion in transition metal dichalcogenides, *2D Materials* **8**, 015030 (2021-01-01).
 - [6] X. X. Zhang, Y. You, S. Y. F. Zhao, and T. F. Heinz, Experimental evidence for dark excitons in monolayer WSe₂, *Physical Review Letters* **115**, 257403 (2015-12-15), publisher: American Physical Society.
 - [7] C. Jin, E. Y. Ma, O. Karni, E. C. Regan, F. Wang, and T. F. Heinz, Ultrafast dynamics in van der waals heterostructures, *Nature Nanotechnology* **13**, 994 (2018), publisher: Springer US.
 - [8] Y. Tang, K. F. Mak, and J. Shan, Long valley lifetime of dark excitons in single-layer WSe₂, *Nature Communications* **10**, 4047 (2019-12-06), publisher: Nature Publishing Group.
 - [9] A. Steinhoff, M. Florian, M. Rösner, G. Schönhoff, T. O. Wehling, and F. Jahnke, Exciton fission in monolayer transition metal dichalcogenide semiconductors, *Nature Communications* **8**, 1166 (2017-12-27), publisher: Nature Publishing Group.
 - [10] J. Wang, J. Ardelean, Y. Bai, A. Steinhoff, M. Florian,

- F. Jahnke, X. Xu, M. Kira, J. Hone, and X. Y. Zhu, Optical generation of high carrier densities in 2d semiconductor heterobilayers, *Science Advances* **5**, 10.1126/sciadv.aax0145 (2019-09-13), publisher: American Association for the Advancement of Science.
- [11] Z. Wang, D. A. Rhodes, K. Watanabe, T. Taniguchi, J. C. Hone, J. Shan, and K. F. Mak, Evidence of high-temperature exciton condensation in two-dimensional atomic double layers, *Nature* **574**, 76 (2019-10-03).
- [12] D. Schmitt, J. P. Bange, W. Bennecke, A. AlMutairi, G. Meneghini, K. Watanabe, T. Taniguchi, D. Steil, D. R. Luke, R. T. Weitz, S. Steil, G. S. M. Jansen, S. Brem, E. Malic, S. Hofmann, M. Reutzler, and S. Mathias, Formation of moiré interlayer excitons in space and time, *Nature* **608**, 499 (2022-08-18).
- [13] J. Madéo, M. K. Man, C. Sahoo, M. Campbell, V. Pareek, E. L. Wong, A. Al-Mahboob, N. S. Chan, A. Karmakar, B. M. K. Mariserla, X. Li, T. F. Heinz, T. Cao, and K. M. Dani, Directly visualizing the momentum-forbidden dark excitons and their dynamics in atomically thin semiconductors, *Science* **370**, 1199 (2020-12-04), publisher: American Association for the Advancement of Science, 2005.00241.
- [14] R. Wallauer, R. Perea-Causin, L. Münster, S. Zajusch, S. Brem, J. Güdde, K. Tanimura, K.-Q. Lin, R. Huber, E. Malic, and U. Höfer, Momentum-resolved observation of exciton formation dynamics in monolayer WS₂, *Nano Letters* **21**, 5867 (2021-07-14), publisher: UTC.
- [15] E. Y. Paik, L. Zhang, G. W. Burg, R. Gogna, E. Tutuc, and H. Deng, Interlayer exciton laser of extended spatial coherence in atomically thin heterostructures, *Nature* **576**, 80 (2019-12-05), publisher: Nature Publishing Group.
- [16] M. Massicotte, P. Schmidt, F. Violla, K. G. Schädler, A. Reserbat-Plantey, K. Watanabe, T. Taniguchi, K. J. Tielrooij, and F. H. L. Koppens, Picosecond photoreponse in van der waals heterostructures, *Nature Nanotechnology* **11**, 42 (2016-01-05).
- [17] M. Massicotte, F. Violla, P. Schmidt, M. B. Lundeberg, S. Latini, S. Haastrup, M. Danovich, D. Davydovskaya, K. Watanabe, T. Taniguchi, V. I. Fal'ko, K. S. Thygesen, T. G. Pedersen, and F. H. Koppens, Dissociation of two-dimensional excitons in monolayer WSe₂, *Nature Communications* **9**, 1 (2018), ISBN: 4146701803864, 1804.07355.
- [18] A. R. Klots, A. K. Newaz, B. Wang, D. Prasai, H. Krzyzanowska, J. Lin, D. Caudel, N. J. Ghimire, J. Yan, B. L. Ivanov, K. A. Velizhanin, A. Burger, D. G. Mandrus, N. H. Tolk, S. T. Pantelides, and K. I. Bolotin, Probing excitonic states in suspended two-dimensional semiconductors by photocurrent spectroscopy, *Scientific Reports* **4**, 1 (2014).
- [19] H. Wang, C. Zhang, W. Chan, S. Tiwari, and F. Rana, Ultrafast response of monolayer molybdenum disulfide photodetectors, *Nature Communications* **6**, 6 (2015), publisher: Nature Publishing Group, 1510.02166.
- [20] S. Ovesen, S. Brem, C. Linderålv, M. Kuisma, T. Korn, P. Erhart, M. Selig, and E. Malic, Interlayer exciton dynamics in van der waals heterostructures, *Communications Physics* **2**, 10.1038/s42005-019-0122-z (2019), publisher: Springer US.
- [21] P. Rivera, K. L. Seyler, H. Yu, J. R. Schaibley, J. Yan, D. G. Mandrus, W. Yao, and X. Xu, Valley-polarized exciton dynamics in a 2d semiconductor heterostructure, *Science* **351**, 688 (2016-02-12), publisher: American Association for the Advancement of Science.
- [22] A. Kumar, D. Yagodkin, N. Stetzuhn, S. Kovalchuk, A. Melnikov, P. Elliott, S. Sharma, C. Gahl, and K. I. Bolotin, Spin/valley coupled dynamics of electrons and holes at the MoS₂–MoSe₂ interface, *Nano Letters* **21**, 7123 (2021-09-08).
- [23] F. Ceballos, M. Z. Bellus, H.-Y. Chiu, and H. Zhao, Ultrafast charge separation and indirect exciton formation in a MoS₂–MoSe₂ van der waals heterostructure, *ACS Nano* **8**, 12717 (2014-12-23).
- [24] E. Y. Ma, B. Guzelturk, G. Li, L. Cao, Z. X. Shen, A. M. Lindenberg, and T. F. Heinz, Recording interfacial currents on the subnanometer length and femtosecond time scale by terahertz emission, *Science Advances* **5**, 10.1126/sciadv.aau0073 (2019-02-08), publisher: American Association for the Advancement of Science.
- [25] H. Wang, C. Zhang, and F. Rana, Ultrafast dynamics of defect-assisted electron–hole recombination in monolayer MoS₂, *Nano Letters* **15**, 339 (2015-01-14), publisher: UTC.
- [26] H. Qiu, T. Xu, Z. Wang, W. Ren, H. Nan, Z. Ni, Q. Chen, S. Yuan, F. Miao, F. Song, G. Long, Y. Shi, L. Sun, J. Wang, and X. Wang, Hopping transport through defect-induced localized states in molybdenum disulphide, *Nature Communications* **4**, 2642 (2013-12-23), publisher: Nature Publishing Group.
- [27] J. Jadczyk, L. Bryja, J. Kutrowska-Girzycka, P. Kapuściński, M. Bieniek, Y.-S. Huang, and P. Hawrylak, Room temperature multi-phonon upconversion photoluminescence in monolayer semiconductor WS₂, *Nature Communications* **10**, 107 (2019-12-10), publisher: Nature Publishing Group.
- [28] A. Alkauskas, Q. Yan, and C. G. Van de Walle, First-principles theory of nonradiative carrier capture via multiphonon emission, *Physical Review B* **90**, 075202 (2014-08-18).
- [29] D. K. Ferry, First-order optical and intervalley scattering in semiconductors, *PHYSICAL REVIEW B* **14** (1976).
- [30] C. Robert, D. Lagarde, F. Cadiz, G. Wang, B. Lassigne, T. Amand, A. Balocchi, P. Renucci, S. Tongay, B. Urbaszek, and X. Marie, Exciton radiative lifetime in transition metal dichalcogenide monolayers, *Physical Review B* **93**, 205423 (2016-05-12), publisher: American Physical Society, 1603.00277.
- [31] J. Zhang, H. Hong, J. Zhang, H. Fu, P. You, J. Lischner, K. Liu, E. Kaxiras, and S. Meng, New pathway for hot electron relaxation in two-dimensional heterostructures, *Nano Letters* **18**, 6057 (2018-09-12), publisher: UTC.
- [32] Z. Nie, R. Long, L. Sun, C.-C. Huang, J. Zhang, Q. Xiong, D. W. Hewak, Z. Shen, O. V. Prezhdo, and Z.-H. Loh, Ultrafast carrier thermalization and cooling dynamics in few-layer MoS₂, *ACS Nano* **8**, 10931 (2014-10-28).
- [33] F. Wu, T. Lovorn, and A. H. MacDonald, Theory of optical absorption by interlayer excitons in transition metal dichalcogenide heterobilayers, *Physical Review B* **97**, 035306 (2018-01-22).
- [34] H. Yu, Y. Wang, Q. Tong, X. Xu, and W. Yao, Anomalous light cones and valley optical selection rules of interlayer excitons in twisted heterobilayers, *Physical Review Letters* **115**, 187002 (2015-10-30), publisher: American Physical Society.
- [35] Y. Jiang, S. Chen, W. Zheng, B. Zheng, and A. Pan,

- Interlayer exciton formation, relaxation, and transport in TMD van der waals heterostructures, *Light: Science and Applications* **10**, 10.1038/S41377-021-00500-1 (2021-12-01), publisher: Springer Nature.
- [36] A. T. Hanbicki, H.-J. Chuang, M. R. Rosenberger, C. S. Hellberg, S. V. Sivaram, K. M. McCreary, I. I. Mazin, and B. T. Jonker, Double indirect interlayer exciton in a MoSe₂/WSe₂ van der waals heterostructure, *ACS Nano* **12**, 4719 (2018-05-22), publisher: UTC.
- [37] H. Wang, C. Zhang, and F. Rana, Surface recombination limited lifetimes of photoexcited carriers in few-layer transition metal dichalcogenide MoS₂, *Nano Letters* **15**, 8204 (2015-12-09).
- [38] Z. Chi, H. Chen, Z. Chen, Q. Zhao, H. Chen, and Y.-X. Weng, Ultrafast energy dissipation *via* coupling with internal and external phonons in two-dimensional MoS₂, *ACS Nano* **12**, 8961 (2018-09-25).
- [39] S. Kar, Y. Su, R. R. Nair, and A. K. Sood, Probing photoexcited carriers in a few-layer MoS₂ laminate by time-resolved optical pump-terahertz probe spectroscopy, *ACS Nano* **9**, 12004 (2015-12-22).
- [40] M. Pandey, F. A. Rasmussen, K. Kuhar, T. Olsen, K. W. Jacobsen, and K. S. Thygesen, Defect-tolerant monolayer transition metal dichalcogenides, *Nano Letters* **16**, 2234 (2016-04-13), publisher: American Chemical Society.
- [41] P. Merkl, F. Mooshammer, P. Steinleitner, A. Girnghuber, K. Q. Lin, P. Nagler, J. Holler, C. Schüller, J. M. Lupton, T. Korn, S. Ovesen, S. Brem, E. Malic, and R. Huber, Ultrafast transition between exciton phases in van der waals heterostructures, *Nature Materials* **18**, 691 (2019), publisher: Springer US, 1910.03890.
- [42] H. Chen, X. Wen, J. Zhang, T. Wu, Y. Gong, X. Zhang, J. Yuan, C. Yi, J. Lou, P. M. Ajayan, W. Zhuang, G. Zhang, and J. Zheng, Ultrafast formation of interlayer hot excitons in atomically thin MoS₂/WS₂ heterostructures, *Nature Communications* **7**, 1 (2016-08-19), publisher: Nature Publishing Group.